

Embedding of SMD populated circuits into FDM printed objects

Florens Wasserfall

*Department of Informatics, Group TAMS, University of Hamburg,
Hamburg, Germany*

REVIEWED

Abstract

This paper introduces the concept of a highly integrated 3D-printing device which is capable of printing plastic parts with integrated, fully assembled electronic circuits in a single process. It is based on a standard FDM 3D-printer that has been augmented by a screw-driven conductive paste extruder for electronic circuit printing, a vacuum nozzle to pick and place SMD-components and a vision system to find and precisely align the components before placing. To control the printer, an existing host software system has been extended to synchronize the communication with the printer for interactive operations and to generate the required movements from camera data by means of image processing.

A number of objects, containing circuits on both the surface and inside of the object, has been successfully printed already. Quality and durability of the generated parts have been evaluated by analyzing the curing characteristics of the conductive ink during the process and the adhesion of the components which are placed directly on the wet ink. The design concept aims for a practical, affordable approach that can be widely used by developers to lower the entrance barrier to the field of 3D-printed electronics. Hence, the hardware is kept as simple as possible, avoiding complex and expensive components as laser or CNC-milling devices, focusing on algorithmic improvements in the preprocessing and control software. All developed hard- and software-components are available under open source licenses and compatible to common existing projects.

1. Introduction

Integrating electronic circuits has the potential to transform additively manufactured parts from pure mechanical objects into "intelligent devices" by embedding sensors, actuators and controllers directly into the three-dimensional structure. A broad variety of approaches has been introduced over the last 15 years to address the integration of circuits into the Additive Manufacturing-process. The direct write approach has been successfully applied in combination with SLA fabrication to produce magnetic flux sensors for the CubeSat project [3, 6, 10], LM555 timer based demonstrators [13, 10] and a highly integrated gaming die, containing a 3-axis accelerometer and several LEDs at the surface to indicate the result of a throw [11]. The focus is set to the advantages of three-dimensional component placement for applications that require a certain orientation e.g. to cover all three orthogonal dimensions of a magnetic field. While the printing of conductive material is more or less automated, placing of components requires manual assistance. Several approaches have been reported to combine the FDM process with different conductive materials: integration of wires [1, 4], airbrush application of coating inks [14], deposition of several low melting metal

alloys [15, 12], direct writing of conductive silver ink [4] and carbon filled plastic filament, called "Carbomorph" [9]. Fundamental issues with the integration of external objects into the printing process have been considered from a general process-planning perspective [2] and evaluated for powder based printers [5].

Based on this groundwork of research, the next consequent step is the integration of the entire process, including the assembling of electronics, into a single device. The FDM technology is considered to be well suited for integration of multiple materials and parts for several reasons: the surface is always flat and open during the build process, no liquids or powders are covering the workspace, interruption and resuming of the print is possible without cleaning or registration of the workpiece. FDM technology is comparably cheap and widely available, increasing the number of potential users. As stated in [4], printing conductive material directly on FDM-generated surfaces is subject to physical constraints. The distortion caused by the surface roughness significantly limits the achievable line width and increases the risk of broken connections. The authors propose a combination of additive FDM manufacturing and subtractive CNC milling to achieve a sufficient quality. However, as demonstrated in this paper, the resolution is at least sufficient for large package sizes such as the 1.27-pitch SOIC package used for the experiments, and can be potentially improved by aligning the print direction of the previous layer with the conductive trace.

2. Description of the printer

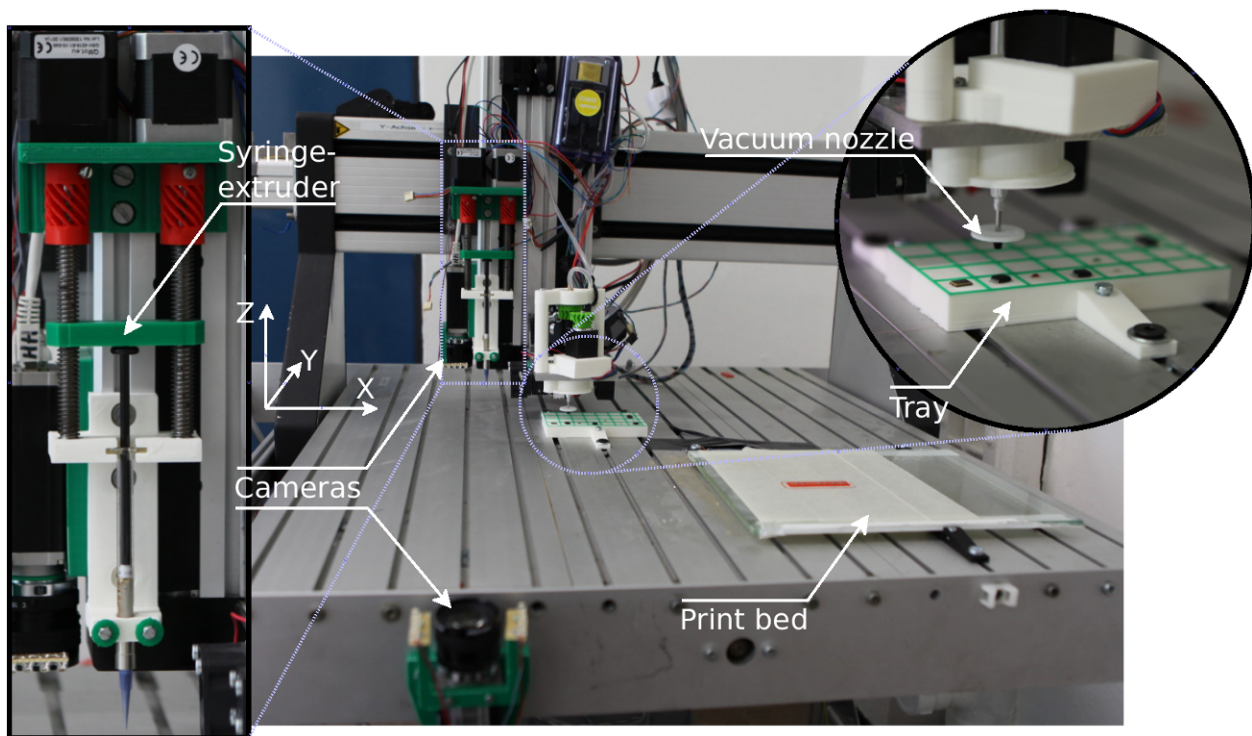


Figure 1 – First iteration of the printing system, based on a CNC milling device.

The first iteration of the introduced printer is based on a CNC cutter with modified driver software to gain compatibility with existing control software (fig. 1). The printer can be controlled by any common host software. It is equipped with a direct driven filament extruder, a syringe extruder for conductive paste processing and a pivot-mounted vacuum nozzle to grip, rotate and place SMD-components. Prior to the printjob, the components are placed manually on a tray that is mounted at the same level as the printed. The tray's surface is divided into boxes by a raised rim. Each component is placed in a single box. This design enables developers to quickly create single prototypes without the need to obtain and handle large belt feeding systems. As described in section 4, the known box dimension is used by the vision system as a reference frame for self calibration. Two cameras are attached to provide vision for the object handling. One is mounted at the printhead, next to the extruders, facing downwards to locate the position of objects on the tray (top camera). The second is mounted at the bed, facing upwards to correct the position and alignment of objects at the vacuum nozzle (bottom camera).

All additional hardware parts are either widely available standard components or designed to be manufactured with a 3D-printer. The design is intended to be as modular and parametric as possible to enable researchers and developers to reuse and adapt it to their requirements and existing hardware setup. The general procedure of printing a single plastic object including a functional circuit is depicted in fig. 2.

3. Characteristics of the direct write extruder

A screw driven syringe extruder is used to print the conductive material. The extruder consists of a gas-tight glass syringe, two motors, ball bearings a few screws and a number of printed parts. All components are comparably cheap and worldwide easy to obtain.

Two conductive materials have been successfully printed with the extruder: In51Bi32Sn16 (Field's metal) and silver filled polymer ink (#6130F, Methode Electronics Inc.). While In51Bi32Sn16 has a generally higher conductivity, a number of negative properties are prevailing. As stated in [15], the surface tension of liquid metal is very high, resulting in bulky traces and preventing the nozzle to disconnect from the floating material without strong oozing effects. Besides, the bonding between the metal and the plastic object proved to be insufficient. In previous work, lead based alloy has been extruded on PCL plastic by [8], but the bonding test was applied against a PCB surface only.

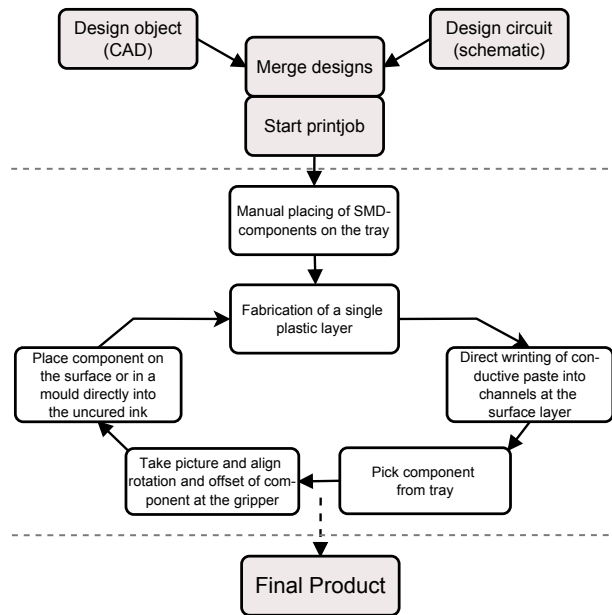


Figure 2 – General process cycle for the fabrication of one object with integrated circuit. White fields indicate steps actually executed by the printer hardware, gray steps are pre- and postprocessing.

In contrast, the #6130F polymer ink shows excellent bonding and extrusion characteristics. The sheet resistance is $40 \text{ m}\Omega/\square$ as stated by the manufacturer. It was expected that the curing characteristics of ink completely enclosed in plastic might be insufficient for more sophisticated circuits. To evaluate this issue, a number of test patterns was printed on an open surface and covered by plastic. The resistance of a $10 \text{ mm} \times 0.5 \text{ mm} \times 0.25 \text{ mm}$ trace was measured over time at room temperature (20°C) and in a heated chamber (60°C). The results are shown in fig. 3 and indicate that the curing is primarily determined by the temperature.

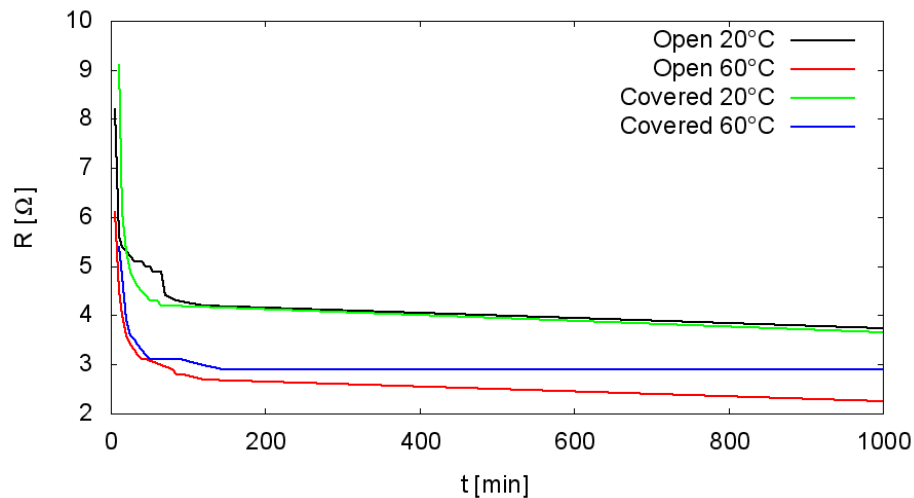


Figure 3 – Curing characteristics of #6130F polymer ink. The resistance of a $10 \text{ mm} \times 0.5 \text{ mm} \times 0.25 \text{ mm}$ trace printed on both the surface of an object and entirely enclosed in plastic is measured during the curing process at room temperature (20°C) and in a heated chamber (60°C).

Depending on the nozzle, a line width of 0.7-0.2 mm is achievable by the extruder on a smooth surface. A line width of 0.2-0.3 mm is desired for fine pitch package sizes (e.g. TSOP). Currently, a line width of 0.5 mm can be reliably achieved on a printed surface. Smaller traces are subject to disruptions caused by bruises in the printed object. Besides, the line width is limited by the large amount of ink required to ensure adhesion of the parts as described in section 6.1.

4. Vision aided pick and place

The tray design described in section 2 requires active detection of parts for the gripping process. This is currently achieved by a system of two cameras. In principle, it would be sufficient to use only one camera for both object localization and alignment, while the object lies on the tray, but the second camera significantly improved the precision in our experiments. The two main reasons for this effect are:

- the objects shift while the printhead moves the vacuum nozzle from the camera position to the part due to vibrations.
- The vacuum nozzle is not accurately rotational symmetric or at least loses its calibration after a few minutes of operation.

In both cases, rotating the part results in massive offsets leading to misplaced components.

4.1. Pick

SMD-parts must be placed on the tray by a human operator prior to a printjob. The rotation must be within a range of $\pm 45^\circ$ since the vision system is not aware of the objects absolute rotation, e.g. the polarity of a diode.

The tray boxes can be used as a reference frame to locate the objects, requiring only a rough calibration of the top camera. The rim of a certain box is extracted by running a Canny line detector (fig. 4 left center) followed by a Hough transform (fig. 4 right center) constrained to a line length of

$$l > \frac{box_size}{2} \text{ and a line orientation of } \theta = \begin{cases} 0^\circ \pm \varepsilon \\ 90^\circ \pm \varepsilon \end{cases} .$$

Cropping the image to the minimal bounding box of these resulting lines extracts a white background square with a known edge length of *box_size*. In a last step, the position of the SMD-part is obtained by computing the histogram and using the minima as the objects center of mass in relation to the tray coordinates (fig. 4 right).

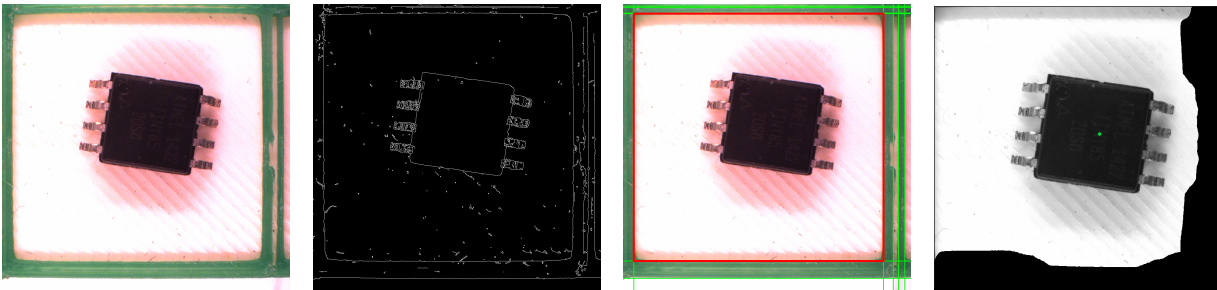


Figure 4 – Image processing steps to locate a single SMD-object in a given tray box. From left to right: raw image provided by the top camera, edges extracted by Canny detector, relevant lines filtered by Hough transform (green) and minimal bounding box (red), objects center of mass from histogram.

4.2. Place

Placing an object requires accurate alignment, which can not be achieved by the human operator while preparing the parts on the tray. Again, Hough line detection is used to find prominent features of the given object. A good threshold for the Hough algorithms accumulator can be determined by the expected size of the object from the extended gcode (section 5.2) or from the area covered by the object after separation from background. The Canny hysteresis threshold window is opened iteratively, starting with a high value, to adaptively find only the most prominent edges (fig. 5).

In a second step the object is rotated to the desired placing orientation. This can induce a significant deviation if the object is not exactly gripped at its center or if the vacuum nozzle is not exactly rotational symmetric (cheap hardware). Therefore, the objects' center of mass is computed again from a second picture, taken after the rotation, to correct this effect. Implementing this in software allows the hardware to be quite imprecise and cheap while still achieving high accuracy. The part is then "impressed" to its destination with a small negative Z-offset to ensure a strong adhesion.

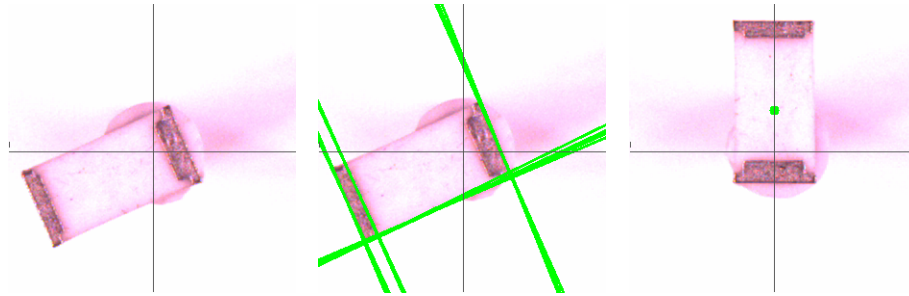


Figure 5 – Image processing steps to align an SMD-part and to correct offsets caused by prior processing steps. From left to right: raw image provided by the bed camera, main features of the object to determine orientation, object in target orientation (90°) and highlighted center of mass. The crosshairs indicate the vacuum nozzles pivot point.

5. Host software

Conventional FDM-printers are usually operated by a realtime capable firmware, which directly controls motors, heaters etc. and a host software, running on a full-sized computer which interacts with the user and feeds the gcode to the firmware. This mainly requires unidirectional, linear communication. The extensions required to control the interactive pick-and-place system are implemented as a plugin for the Octoprint [7] host software. Both, Octoprint and the OctoPNP plugin are available under a GPLv3 license.

5.1. Synchronizing the communication

Complex printing geometries are composed of a large number of small linear movements. The firmware usually buffers a number of commands to avoid interrupted movements caused by communication delays. Interacting with external objects during the printing process requires synchronization between the printers firmware and the host controller at some points to complete positioning moves before taking a picture. This is realized by exploiting the `M400` gcode command implemented by several firmwares. The firmware acknowledges every received command until the buffer is filled, and from this point on every time a command has been successfully executed. The `M400` command blocks every acknowledgment messages for non immediately returning operations until it has been executed, causing the buffer to run dry.

5.2. Gcode extensions

Controlling the syringe extruder can be done by simply treating it as a normal extruder with high filament diameter (the syringe-piston diameter) and no heater. However, the vacuum nozzle for part handling relies on the data created interactively by the image processing, making it impossible to pre-compute the gcode commands. The proposed solution, currently implemented in the host software, is to extend the gcode for in-line part description as shown in fig. 6. The XML statements are treated as comments and therefore ignored by a normal gcode interpreter. The part information is preprocessed by the host software to display the box allocation for each part to the user.

```

1 G28
2 G1 X10 Y35 Z14 F3000
3 M361 P4
4
5 ;<part id="1" name="LED-1206">
6 ; <position box="4"/>
7 ; <size height="1.05"/>
8 ; <shape>
9 ; <rect x1="-1.5" y1="0.75" x2="1.5" y2="-0.75"/>
10 ; </shape>
11 ; <pads>
12 ; <pad x1="-1.5" y1="0.75" x2="-1.1" y2="-0.75"/>
13 ; <pad x1="1.5" y1="0.75" x2="1.1" y2="-0.75"/>
14 ; </pads>
15 ; <destination x="104.938" y="27.987" z="8.000" orientation="90"/>
16 ;</part>

```

Figure 6 – XML Gcode extension for in-line description of SMD parts. The M361 command actually executes the placing operation for a certain object, during the printing process. The <shape> and <pads> information is currently used by the host software for visualization of the parts in the user interface. Integrating it as a threshold measure for the Hough algorithm is currently under development.

6. Experimental results

As shown in fig. 7, printing traces and precisely placing components on this traces works reliably on flat surfaces. The orientation of the underlying layer significantly affects the trace quality, causing the "staircase" effect that can be noticed at the bottom of the green LED.

6.1. Bonding characteristics

Since the parts are placed directly into uncured ink, the bonding characteristics are crucial to assess the electrical and mechanical quality of a manufactured object. Besides, this information is relevant for the design of toolpath generators (slicing software).

As shown in fig. 8 (left), a series of specimen was produced on the printer, each containing several 1206 SMD-resistors, placed with increasing time delay on two 0.5 mm ink traces. After a curing period of one day, a shear force was applied to the parts by a calibrated flat spring until the part was released. The results are shown in fig. 8 (right).

The data shows high variance, but a trend is clearly visible. The bonding quality partly depends on the conductive line geometry which varied over time due to several recalibrations of the syringe extruder during the long experiment. The results indicate that a fast placing of parts after the fabrication of a conductive trace is important to achieve reliable connections. A period of up to

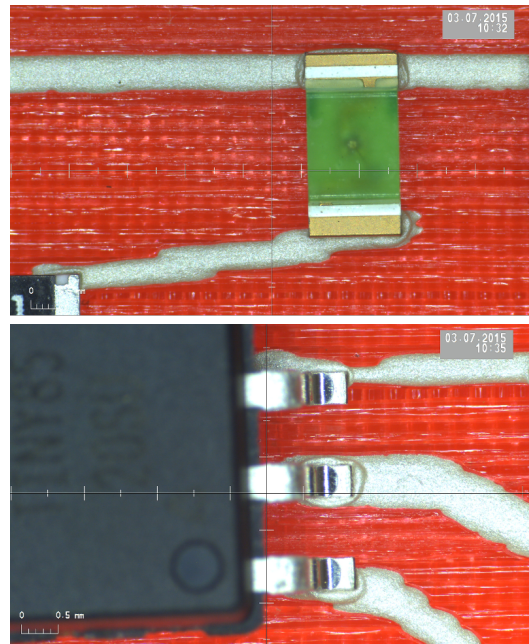


Figure 7 – Bonding and accuracy of SMD parts, correctly placed by the printer.

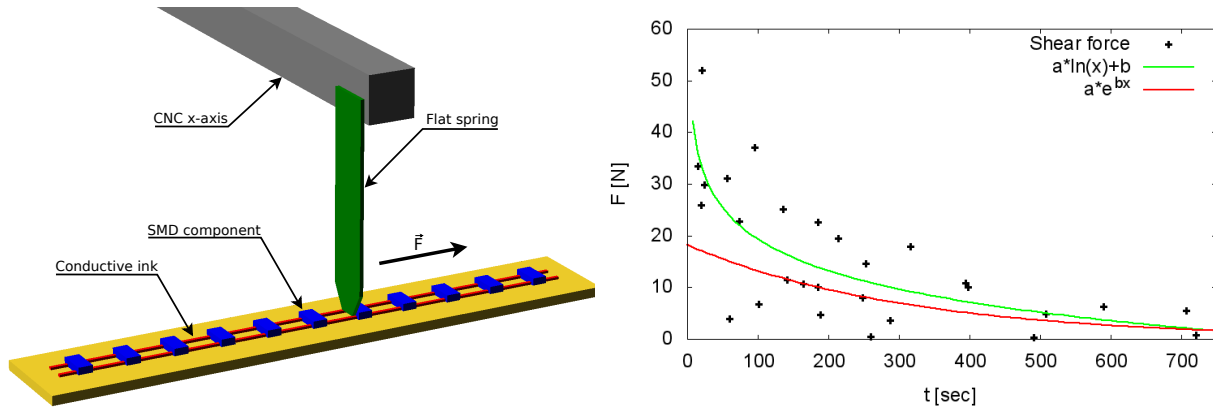


Figure 8 – Evaluation of the bonding quality. Experiment setup to measure shear forces required to release SMD parts from cured ink traces on the surface of printed specimen (left) and results (right). The X-axis indicates the time between finishing the ink trace and placing a part into this trace.

100 seconds for uncovered parts at the objects surface and 200-300 seconds for plastic covered parts is considered to be a reasonable value. This implies that it is not possible to create a trace, continue printing the object and place the part into a left open cavity for most objects, because printing several layers usually requires more than 3 minutes. Potential approaches to mitigate this problem are:

- Embedding the parts upside down and connecting the part by ending the conductive trace on the pad.
- Deposition of small ink droplets on the pin landing areas. This requires an appropriate needle and potentially causes collisions between the plastic extruder and the object since the landing layer is below the objects surface.
- Utilization of conductive ink with slower curing characteristics (e.g. Methode #6130S).

6.2. Printed objects

A number of objects was printed to evaluate different aspects of the behavior of conductive ink inside of FDM-generated objects. Designing objects with integrated electronics currently requires extensive manual labor due to the lack of appropriate design software.

Vertical connections Vertical connections between different layers have been successfully established by printing a wire with 45° inclination which is slightly distorted along the printing orientation to increase the contact area. A test connection printed at the surface for optical inspection is shown in fig. 9 (left) and one of the microcontroller pins in the right image is connected to the objects bottom to establish a connection to the USB ports case.

Surfaces The object in fig. 9 (center) demonstrates the fabrication of free-form conductive surfaces, e.g. to be used as capacitive touch sensors.

SMD populating To demonstrate the automatic placing of parts, a simple object was created, containing an ATtiny 85-20 microcontroller, controlling 2 LEDs (fig. 9 right). The object

directly fits into a USB port. The ATtiny was successfully programmed by a modified programming adapter connected to the USB pins, and the circuit is powered when plugged into a normal USB port.

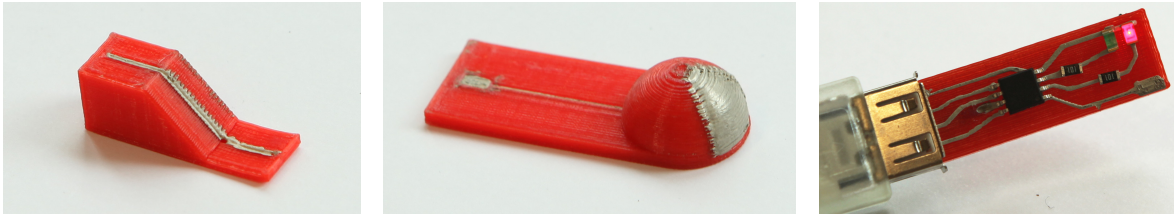


Figure 9 – Printed test objects to demonstrate vertical connections (left), capacitive free-form surfaces (center) and fully populated circuits (right).

7. Conclusion and future work

In this paper, the design of a 3D-printer was successfully demonstrated which is capable of creating complete electronic circuits integrated into printed plastic objects. This is achieved by enhancing a common device with pick and place hardware, controlled by a computer vision system. It shows that it is possible to improve nowadays printing hardware for this task, at costs in the range of $\sim 1000\text{€}$. The design is modular and open, to be compatible to a broad range of hardware setups and applications. This is a basic step to enable researchers to further explore the potential of AM-manufactured functional objects.

Future work includes the transformation of the hardware to "standard" printers and the fabrication of more sophisticated objects. Two important aspects are the integration of sensors and the decentralization of electronics, superseding bulky circuit boards. A focus will be set to the development of design software, supporting the creation and pre-processing of objects. Another interesting subject is increasing the vacuum nozzles DOF to achieve real free-form placing.

More information, including the source code for the OctoPNP software and hardware designs is available on the projects website: https://tams.informatik.uni-hamburg.de/research/3d-printing/conductive_printing.

References

- [1] J. Bayless, M. Chen, and B. Dai. Wire embedding 3d printer, 2010.
- [2] J. Cham, B. Pruitt, M. Cutkosky, M. Binnard, L. E. Weiss, and G. Neplotnik. Layered manufacturing with embedded components: process planning considerations. In *Proceedings of DETC99: 1999 ASME Design Engineering Technical Conference*, pages 1–9, 1999.
- [3] E. De Nava, M. Navarrete, A. Lopes, M. Alawneh, M. Contreras, D. Muse, S. Castillo, E. Macdonald, and R. Wicker. Three-Dimensional Off-Axis Component Placement and Routing for Electronics Integration using Solid Freeform Fabrication. *Proceedings from the 19th Annual Solid Freeform Fabrication Symposium*, pages 362–369, 2008.

- [4] D. Espalin, D. W. Muse, E. MacDonald, and R. B. Wicker. 3d printing multifunctionality: Structures with electronics. *International Journal of Advanced Manufacturing Technology*, 72:963–978, 2014.
- [5] J. Glasschroeder, E. Prager, and M. F. Zaeh. Powder-bed based 3d-printing of function integrated parts. In *Proceedings of SFFS2015: International Solid Freeform Fabrication Symposium*, pages 775–792, 2014.
- [6] C. Gutierrez, R. Salas, G. Hernandez, D. Muse, R. Olivas, E. MacDonald, M. D. Irwin, R. Wicker, K. Churck, M. Newton, and B. Zufelt. CubeSat Fabrication through Additive Manufacturing and Micro-Dispensing. *Proceedings from the IMAPS Symposium*, 2011.
- [7] G. Häußge. Octoprint - generic host software for 3d-printers, project website. <http://octoprint.org>, 2015.
- [8] M.-S. Kim, W.-S. Chu, Y.-M. Kim, A. P. G. Avila, and S.-H. Ahn. Direct metal printing of 3d electrical circuit using rapid prototyping. *International Journal of Precision Engineering and Manufacturing*, 10, 2010.
- [9] S. J. Leigh, R. J. Bradley, C. P. Purcell, D. R. Billson, and D. A. Hutchins. A simple, low-cost conductive composite material for 3d printing of electronic sensors. *PLoS ONE*, 7(11), 11 2012. doi: 10.1371/journal.pone.0049365. URL <http://dx.doi.org/10.1371%2Fjournal.pone.0049365>.
- [10] A. J. Lopes, E. MacDonald, and R. B. Wicker. Integrating stereolithography and direct print technologies for 3D structural electronics fabrication. *Rapid Prototyping Journal*, 18:129–143, 2012. ISSN 1355-2546. doi: 10.1108/13552541211212113.
- [11] E. Macdonald, R. Salas, D. Espalin, M. Perez, E. Aguilera, D. Muse, and R. B. Wicker. 3D printing for the rapid prototyping of structural electronics. *IEEE Access*, pages 234–242, march 2014. doi: 10.1109/ACCESS.2014.2311810.
- [12] J. Mireles, H. Kim, I. H. Lee, D. Espalin, F. Medina, E. MacDonald, and R. Wicker. Development of a fused deposition modeling system for low melting temperature metal alloys. *J. Electron. Packag.*, 135, 2013. doi: 10.1115/1.4007160.
- [13] D. Periard, E. Malone, and H. Lipson. Printing embedded circuits. *Proceedings from the Solid Freeform Fabrication Symposium*, pages 503–512, 2007.
- [14] J. Sarik, A. Butler, N. Villar, J. Scott, and S. Hodges. Combining 3d printing and printable electronics. In *TEI 2012 Works in Progress*. ACM, 2012.
- [15] E. Sells and A. Bowyer. Rapid prototyped electronic circuits. Technical report, University of Bath, Department of Mechanical Engineering, 2004.